Variational calculations of simple Bose systems*

V. R. Pandharipande and K. E. Schmidt
University of Illinois, Urbana, Illinois 61801
(Received 18 October 1976)

Variational calculations of the ground-state energy of hard-sphere, helium-4, Coulomb, and nuclear Yukawa fluids are carried out. The long-range part $v(r > d)$ and a constant part λ at $r < d$ of the bare interaction are assumed to contribute to the average field. The correlation function $f(r)$ is obtained by minimizing the two-body cluster contribution due to the remainder interaction, and the distance d is determined by minimizing the energy as calculated with the hierarchy of hypernetted-chain-type equations. The convergence of two- and three-particle distribution functions given by these equations is discussed. The method is shown to be exact in the low-density limit, and the comparison of the present results with the available exact (standard) results in the high-density limit (region) verifies its accuracy over the entire density range. It is shown that the variationally obtained value of d in the high-density Coulomb fluid can be understood with conventional mean-field theory. A solidification criterion is obtained by studying the energies in liquid and solid phases with the present $f(r)$. This criterion explains the solidification of the Coulomb, hard-sphere, and helium systems, and the inability of the nuclear Yukawa system to solidify. The variational method in the form presented here could be very useful for studying complicated quantum systems.

I. INTRODUCTION

The wave function commonly used in variational calculations of quantum fluids at zero temperature has the form

$$\Psi_v = \prod_{i<j} f_{ij} \Phi , \tag{1.1}$$

where Φ is the ideal noninteracting fluid wave function, and f_{ij} describes the correlation between the particles i and j due to their interaction. The f is varied to minimize the energy. The standard method[1] is to approximate the f by a function of the interparticle distance r,

$$r_{ij} = |\vec{r}_i - \vec{r}_j| , \tag{1.2}$$

choose a suitable form for it,

$$f = \exp(-br^{-a}) , \tag{1.3}$$

for example, calculate the energy expectation value as a function of the parameters in f (a and b in the example) and minimize it. The main advantage of this method is that at least for simple Bose systems, where the two-body potential v is a simple function of r, exact Monte Carlo calculations of an upper bound are possible. Moreover, in these systems one expects on the grounds of symmetry that f is a spherically symmetric function of $\vec{r}$, and hence the calculated upper bound could be close to the true energy provided the chosen algebraic form of f is adequate.

The main disadvantage is that in many systems of interest the correlations cannot be described by a simple function of r. The correlation between two particles in simple Fermi systems can be complex and can depend upon the angle θ between $\vec{r}$ and their relative momentum $\vec{k}$, even when v is a function of r only. In the limit $k \to 0$ the imaginary θ-dependent part of f generates the "back flow" and contributes to the effective mass of particles in fluid media.[2] Also in some dense systems of interest, nuclear[3,4] and neutron-star[5] matter, for example, the v is a complicated operator containing spin-spin, tensor, spin-orbit, and other terms. In such systems the f is also expected to contain significant spin-spin, tensor, spin-orbit, etc., correlations.[4]

There are two problems involved in developing a variational theory of such systems: first, too many parameters are required to describe an f that is sufficiently general, and second, the existing Monte Carlo methods cannot calculate the energy expectation value with a complex f, though in principle it may well be possible to develop numerical integration programs to do so.

A plausible scheme to avoid these problems is suggested in Refs. 4 and 5 (Ref. 5 will henceforth be called PB). PB calculate the f by analytically minimizing the two-body cluster contribution with healing constraints which require the f to be unity beyond a certain distance d. This f contains the back flow[2] and other components[4] dictated by the two-body interaction, and is described by a single parameter d which is its range. The d is obtained by minimizing $E(d)$. In many cases $E(d > 2r_0)$, where r_0 is the unit radius, $4\pi/3r_0^3 = \rho^{-1}$ and ρ the density, simply becomes insensitive to d. Also PB choose to use the hierarchy of hypernetted chain (1.4) equations HNC and HNC/4 to calculate the energy. The diagrammatic techniques under-

lying these equations are particularly suitable for calculating E when f is complicated.[6]

In the present work we study some simple Bose systems [hard sphere (HS), Coulomb (CL), helium-4 (HF), and nuclear Yukawa (NY)] with the methods developed by PB. By nuclear Yukawa we mean a system of bosons having the mass of a nucleon and interacting with a Yukawa potential $29\hbar c e^{-4r}/r$ (r in fm). In Sec. II we discuss the calculation of f and show that the healing constraint approximately simulates the variation of the many-body cluster contributions. The method is also shown to be exact in the low-density limit wherever applicable.

The convergence between HNC and HNC/4, the lowest two orders in the elementary diagram expansion due to van Leeuwen *et al.*,[6] is discussed in Sec. III. General arguments which suggest that the HNC summation of diagrams should be adequate in most cases of interest are given. Earlier studies,[7] in which the energy was calculated only from the two-particle distribution function using the Jackson-Feenberg (JF) identity,[8] indicated that the HNC integral equation is not sufficiently accurate to treat dense systems. Much of the accuracy realized in the present scheme can be attributed to the method of calculating the energy as $W+U$, where W depends upon the two-particle distribution function and includes the potential plus a part of the kinetic energy coming from terms containing $\nabla_i^2 f_{ij}$. The kinetic energy contribution U contains $\nabla_i f_{ij}\cdot\nabla_i f_{ik}$ terms, and depends upon the three-particle distribution function. In Sec. III we suggest an explanation of earlier results[7] with HNC equations by showing that the U is calculated with an erroneous three-body distribution function when the JF identity is used with HNC two-body distribution function.

The present results are compared with the available low-density expansions for HS and CL, high-density expansion for CL, and the Monte Carlo results for high density HS and CL systems in Sec. IV. These comparisons verify the assumptions in the present method. It is found that the healing distance $d(\rho)$, which minimizes the high-density CL energy, corresponds to the range of effective interaction estimated from the static dielectric constant $\epsilon(q,0)$. In Sec. V, we suggest that the PB correlation functions could be useful for studying the solidification of these liquids. Arguments which suggest that solidification should occur when the three-body kinetic energy U in liquids becomes large compared to the localization energy in solids are presented. It is shown that one can qualitatively understand the solidification of CL at low density, that of HS and HF at high density, and the inability of NY to solidify[9] with this criterion.

II. CALCULATION OF f

PB assumes that the long-range part $v(r>d)$ of the two-body interaction contributes only to the average one-body potential. Since it does not induce significant correlations it should be omitted from the calculation of f. A minimization of the two-body cluster contribution (C_2) to the energy with constraint $\hat{f}(r>d)=1$ gives the variational equation:

$$\delta\frac{\rho}{2}\int_0^d \hat{f}\left(-\frac{\hbar^2}{m}\nabla^2\hat{f}+v\hat{f}\right)4\pi r^2\,dr=0 \tag{2.1}$$

which gives the equation for $\hat{f}$:

$$-(\hbar^2/m)\nabla^2\hat{f}+v\hat{f}=0\,. \tag{2.2}$$

The solution of Eq. (2.2) should be normalized so that $\hat{f}(d)=1$, and generally the derivative of $\hat{f}$ is discontinuous at d.

PB eliminates the unphysical discontinuity at d by assuming that a part of the interaction at $r<d$ must also contribute to the average field. It is approximated by a constant λ and subtracted from the variational Eq. (2.1). Solving

$$\delta\frac{\rho}{2}\int_0^d f\left(-\frac{\hbar^2}{m}\nabla^2 f+(v-\lambda)f\right)4\pi r^2\,dr=0 \tag{2.3}$$

gives a Schrödinger-type equation.

$$-(\hbar^2/m)\nabla^2 f+vf=\lambda f\,. \tag{2.4}$$

The λ can now be obtained by requiring the derivative of f to be continuous at d. Even though the C_2 obtained with the continuous f is higher than that with the discontinuous $\hat{f}$, the total energy, which is a sum of C_2 and the many-body-cluster contributions (MBCC), obtained with f is lower than that with $\hat{f}$. The differences between the energies given by f and $\hat{f}$ could be quite small. For example, hard spheres of radius a at density $\rho=0.2a^{-3}$ and $d=2r_0$ give

$$C_2(\hat{f})=2.38<C_2(f)=2.62\,, \tag{2.5}$$

but

$$E(\hat{f})=6.00\gtrsim E(f)=5.99\,. \tag{2.6}$$

The energies are in units of $\hbar^2/ma^2$, and the total E is calculated with the HNC/4 method as discussed in Sec. III.

Equation (2.4) can be obtained variationally without average field arguments by assuming that the variation of the MBCC is proportional to that of the integral of $1-f^2$:

$$\delta(\mathrm{MBCC})\propto\delta\int_0^d(1-f^2)4\pi r^2\,dr\,. \tag{2.7}$$

The MBCC involve integrals containing powers of $1-f^2$, and thus it is plausible that MBCC is a

smooth function of the integral of $1-f^2$. Over a limited region in the neighborhood of the f, one may approximate this function by a straight line whose slope is the constant of proportionality in (2.7). The boundary condition on f determines this slope by assuming that the variation of MBCC makes f heal at $r=d$. The unknown d (or λ) is determined variationally by minimizing $E(d)$.

The above argument, though plausible, cannot be completely true because variations in f which leave the integral over $1-f^2$ invariant do not necessarily leave MBCC invariant. Hence we have attempted to test the validity of Eq. (2.4) by assuming a more general shape for the contribution of the interaction at $r<d$ to the average field. It is taken as

$$\lambda(r<d)=\lambda_0(1+\Lambda r), \tag{2.8}$$

the λ_0 is obtained from the boundary condition, while Λ is an additional variational parameter. Generally at values of d at which $E(\rho, d)$ has a minimum it is found that $E(\rho, d, \Lambda)$ has a very shallow minimum near $\Lambda=0$ and thus $E(\rho,d,\Lambda=0)$ either equals or is extremely close to the energy at the minimum.

It can be easily shown that the equations

$$\frac{\partial E(d)}{\partial d}=0 \tag{2.9}$$

and (2.4) give the exact energy in the low-density limit. Let v have a finite range R and a scattering length a. In the limit $d\geq r\gg a$ the solution of (2.4) becomes

$$f=\frac{\sin k(r-a)}{\sin k(d-a)}\,\frac{d}{r}, \tag{2.10}$$

$$\lambda=(\hbar^2/m)k^2=(\hbar^2/m)3a/d^3. \tag{2.11}$$

At low densities,

$$a\ll d\ll r_0, \tag{2.12}$$

the MBCC may be neglected to obtain

$$E(\rho\to 0)=(\hbar^2/m)2\pi\rho a, \tag{2.13}$$

which is the well-known low-density limit.[10] This low-density limit may also be obtained from the $\hat{f}$ [Eq. (2.2)]; the discontinuity vanishes in the limit $d\to\infty$.

III. CALCULATION OF ENERGY

The energy expectation value can be written

$$E=W+U, \tag{3.1}$$

$$W=\frac{\rho}{2}\int V(r)g(r)4\pi r^2\,dr, \tag{3.2}$$

$$V(r<d)=\lambda, \quad V(r>d)=v(r), \tag{3.3}$$

$$U=-\frac{\hbar^2}{2m}\rho^2\int g_3(\vec{r}_{12},\vec{r}_{13})\frac{\nabla_1 f_{12}}{f_{12}}\cdot\frac{\nabla_1 f_{13}}{f_{13}}\,d^3r_{12}\,d^3r_{13}. \tag{3.4}$$

The $g(r)$ and $g_3(\vec{r}_{12},\vec{r}_{13})$ are two- and three-particle distribution functions which can be expanded in powers of $F(r)$,

$$F(r)=f^2(r)-1. \tag{3.5}$$

Each term in the expansion can be represented by a diagram[5,6] in which a dashed line represents the function F. The diagrams are classified as composite, nodal, and elementary[6]; the integral equation

$$\ln\left(\frac{g_{mn}}{f^2_{mn}e^{E_{mn}}}\right)=\rho\int\left[g_{m_1}-1-\ln\left(\frac{g_{m_1}}{f^2_{m_1}e^{E_{m_1}}}\right)\right](g_{n_1}-1)\,d^3r_1 \tag{3.6}$$

sums all composite and nodal diagrams formed from the elementary diagrams included in E_{mn}. Following PB we denote the variables of the function by subscripts, thus

$$g_{mn}\equiv g(r_{mn})\equiv g(|\vec{r}_m-\vec{r}_n|). \tag{3.7}$$

In the approximation $E_{mn}=0$ we get the familiar HNC (hypernetted chain) integral equation which sums the diagrams illustrated in Fig. 1. In this

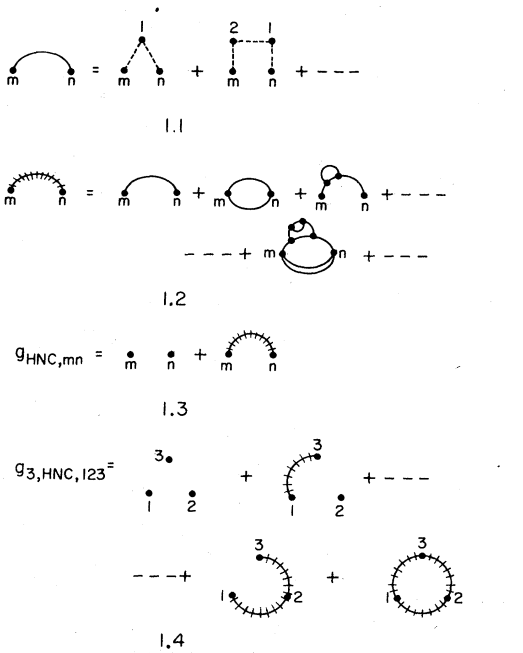

FIG. 1. Diagrams 1.1 and 1.2, respectively, define the sum of all single chain and hypernetted chain diagrams, while diagrams 1.3 and 1.4 give the g_{HNC} and $g_{3,HNC}$.

approximation g_3 is merely given by superposition

$$g_{3,\mathrm{HNC},123} = g_{\mathrm{HNC},12}\, g_{\mathrm{HNC},23}\, g_{\mathrm{HNC},31}\,, \tag{3.8}$$

as illustrated in Fig. 1 diagram 1.4.

To test the validity of the HNC approximation, PB solved Eq. (3.6) in "HNC/4" approximation with the E_{mn} given by the first elementary diagram (the four-body diagram 2.1 shown in Fig. 2),

$$E_{\mathrm{PB},mn} = \tfrac{1}{2}\rho^2 \int F_{m1} F_{m2} F_{n1} F_{n2} F_{12}\, d^3r_1\, d^3r_2\,. \tag{3.9}$$

However, using arguments presented in Sec. IV of PB it can be shown that many elementary diagrams (2.2, for example) are comparable to 2.1. Thus the PB choice of E_{mn} is not very satisfactory. In the present work E_{mn} in the HNC/4 equation is taken to be

$$E_{mn} = \tfrac{1}{2}\rho^2 \int G_{m1} G_{m2} G_{n1} G_{n2} G_{12}\, d^3r_1\, d^3r_2\,, \tag{3.10}$$

$$G_{ij} = g_{\mathrm{HNC},ij} - 1\,. \tag{3.11}$$

The function G_{ij} is represented by a double line, and its diagrammatic equivalence is shown in Fig. 2 diagram 2.3. The diagram 2.4 contains the sum

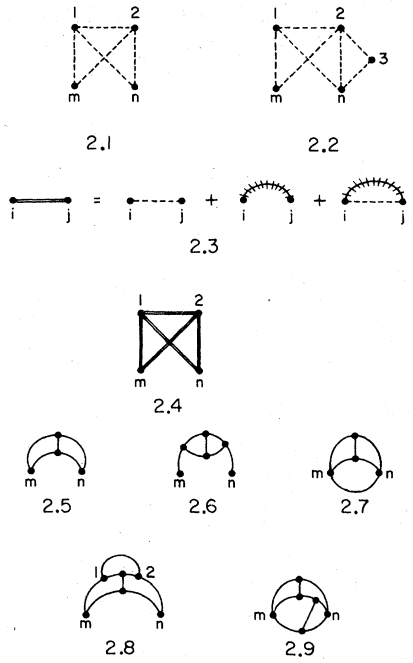

FIG. 2. Elementary diagrams that have a single coupling between two single chains are shown in diagrams 2.1 and 2.2, while diagram 2.3 gives the diagrammatic equivalence of function G. Diagram 2.4 gives the sum of all diagrams in which two hypernetted chains linking m and n are coupled by either an F or a HNC or both. Diagrams of type 2.5–2.7 contribute to the difference δg, while those of type 2.8–2.9 are omitted in $g_{\mathrm{HNC}/4}$.

of 2.1 and all other elementary diagrams that can be comparable to 2.1.

The simplest type of diagrams contained in the difference δg,

$$\delta g = g_{\mathrm{HNC}/4} - g_{\mathrm{HNC}} \tag{3.12}$$

are shown in Fig. 2 diagrams 2.5–2.7. The simplest type of diagrams omitted in HNC/4 have structures of the type in diagrams 2.8–2.9. Diagrams of type 2.8 are simply those of type 2.5 with an additional chain linking particles 1 and 2. Summing all possible chains linking 1 and 2 gives the function G_{12}, and thus integrals represented by diagrams 2.8 have an extra G_{12} compared to those represented by diagrams 2.5. Since generally $G \leqslant 1$ we can expect the contributions of diagram 2.8 to be smaller than those of diagram 2.5. Such arguments suggest that the diagrams neglected by HNC/4 with E_{mn} given by (3.10) are smaller than those contributing to δg, (for example, diagrams 2.9 are less than diagrams 2.7, etc.).

We now give plausibility arguments which suggest that in most cases of interest we should not expect δg to be more than a few percent of g_{HNC}. The Fourier transform of the HNC equation gives

$$L(k) = \rho^2 G^2(k)/[1 + \rho G(k)]\,, \tag{3.13}$$

where $L(k)$ and $G(k)$ are Fourier transform of $\ln(g/f^2)$ and $G(r)$, respectively. It is necessary that

$$\rho G(k) > -1 \tag{3.14}$$

for Eq. (3.13) to have a solution. The above equation at $k = 0$ imposes a lower bound on the volume integral of G.

$$4\pi\rho \int_0^\infty G(r) r^2\, dr > -1\,. \tag{3.15}$$

Since $g(r)$ is positive definite $G(r) \geqslant -1$. When the potential contains a strong repulsive core $G(r < r_0) \approx -1$ and $G(r > r_0)$ fluctuates around zero. Assuming that the fluctuating part gives negligible contribution we could estimate $E_{mn}(r_0)$ with an approximate $\overline{G}$,

$$\overline{G}(r < r_0) = -1, \quad \overline{G}(r > r_0) = 0\,, \tag{3.16}$$

which corresponds to the maximum permissible hole.

$$E_{mn}(r_0) < \tfrac{1}{2}\rho^2 \left(\int \overline{G}_{m1} \overline{G}_{n1}\, d^3r_1 \right)^2 = \tfrac{1}{2}\left(\tfrac{5}{16}\right)^2 \approx 0.05\,. \tag{3.17}$$

The estimated $E_{mn}(r_0)$ in this case is around 0.025. The $E_{mn}(r \approx 0)$ could be larger (≈ 0.25) but it is inconsequential because $f^2(r \approx 0)$ is practically zero.

As another extreme case (high-density Coulomb gas, for example) one could estimate E_{mn} with a

long range G. Again the magnitude of G must be smaller than $(r_0/D)^3$ if D is its range (neglecting the fluctuating part). In such cases the E_{mn} is very small, for example, if $D=2r_0$, $E_{mn}(0)<10^{-3}$. A study of δg diagrams reveals that when $E_{mn}(r)\ll 1$ $\delta g(r)\approx E_{mn}(r)f^2(r)$ and thus $\delta g(r)$ may be expected to be a few percent of $g_{\rm HNC}$ in most cases of interest.

The contribution of the four-body elementary diagram 2.1 by itself can be larger because the volume integral of F does not have a lower bound of type Eq. (3.15). Thus the contribution of diagram 2.1 is not a good criterion to examine the accuracy of $g_{\rm HNC}$. Recently Smith[11] has approximately studied the convergence between HNC, HNC/4, and HNC/5 using four- and five-body elementary diagrams with both F and G functions. The expansion using elementary diagrams calculated with G's has better convergence than that with F functions.

We note that for the exact distribution function, correct to terms of order $1/\Omega$, where Ω is the volume of the system, Eq. (3.15) is an equality. However in obtaining an irreducible cluster expansion terms of order $1/\Omega$ are neglected, and hence even if all the diagrams were to be summed Eq. (3.15) may not become an equality. For example when $f=1$ all diagrams give zero contribution, $g(r)=1$ and $G(r)=0$. This g satisfies Eq. (3.15) as an inequality, but not as an equality. In the literature the G has been at times required to satisfy Eq. (3.15) as an equality, which we believe could be erroneous while working with irreducible cluster expansions.

The g_3 consistent with approximations in HNC/4 is given by

$$g_{3,\mathrm{HNC/4},123}=g_{\mathrm{HNC/4},12}\,g_{\mathrm{HNC/4},23}\,g_{\mathrm{HNC/4},31}\times\left(1+\rho\int G_{1m}G_{2m}G_{3m}\,d^3r_m\right). \tag{3.18}$$

PB neglected the second term of $g_{3,\mathrm{HNC/4}}$ which violates the superposition approximation. Equation (3.6) is first solved with $E_{mn}=0$ to calculate the G. We then calculate the E_{mn} using Eq. (3.10) and solve (3.6) again to obtain $g_{\mathrm{HNC/4}}$, from which $g_{3,\mathrm{HNC/4}}$ is obtained with Eq. (3.18).

Earlier studies,[7] in which the energy was calculated from only the two-particle distribution function using the Jackson-Feenberg (JF) identity,[8] indicated that the HNC integral equation is not sufficiently accurate to treat dense systems. We will now demonstrate the basis for problems associated with using the JF identity along with elementary diagram expansions.

With JF identity the energy can be written as

$$E_{\rm JF}=\frac{\rho}{2}\int V_{\rm JF}(r)\,g(r)\,4\pi r^2\,dr, \tag{3.19}$$

$$V_{\rm JF}(r<d)=\tfrac{1}{2}\left[v+\lambda_0+(\hbar^2/m)(\nabla f)^2/f^2\right], \tag{3.20}$$

$$V_{\rm JF}(r>d)=v(r). \tag{3.21}$$

The difference between $E_{\rm JF}$ and W is obtained as

$$E_{\rm JF}-W=\frac{\rho}{2}\int\frac{\hbar^2}{2m}\left(\frac{\nabla_m^2 f_{mn}}{f_{mn}}+\frac{(\nabla_m f_{mn})^2}{f_{mn}^2}\right)g_{mn}\,d^3r$$
$$=\frac{\rho}{2}\int\frac{\hbar^2}{2m}\left(\frac{2(\nabla_m f_{mn})^2}{f_{mn}^2}\,g_{mn}-\frac{\nabla_m f_{mn}}{f_{mn}}\cdot\nabla_m g_{mn}\right)d^3r. \tag{3.22}$$

Now the g_{mn} can be written as f_{mn}^2 (1 +diagram contributions). By letting the ∇_m in the second term operate on the f_{mn}^2 in g_{mn} we get a term that exactly cancels the first term in (3.22). Thus

$$E_{\rm JF}-W=-\frac{\rho}{2}\,\frac{\hbar^2}{2m}\int f_{mn}\nabla_m f_{mn}\circ\nabla_m\ \text{(diagram contributions)}. \tag{3.23}$$

In principle $E_{\rm JF}-W$ should simply be U, and it is easy to see, by differentiating the contribution of some of the g diagrams, that one simply obtains diagrams that contribute to U. For example, by differentiating the three-body g diagram 3.1 in Fig. 3 we get

$$(E_{\rm JF}-W)_{3\text{-body}}=+\frac{\rho^2}{2}\,\frac{\hbar^2}{m}\int f_{mn}\nabla_m f_{mn}\cdot f_{m_1}\nabla_m f_{m_1}f_{n_1}\,d^2r_{m_1}\cdot d^3r_{mn}$$
$$=-\frac{\rho^2}{2}\,\frac{\hbar^2}{m}\int f_{mn}\nabla_m f_{mn}\cdot f_{m_1}\nabla_m f_{m_1}f_{n_1}^2\,d^3r_{m_1}\,d^3r_{mn}, \tag{3.24}$$

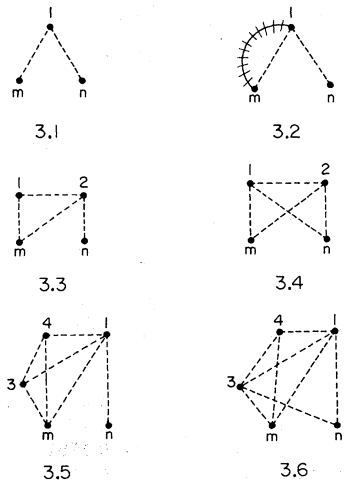

FIG. 3. Some diagrams that contribute to g_{mn}.

TABLE I. Two-particle distribution function in HF at $\rho = 0.365\sigma^{-3}$.

r/r_0	g_{HNC}	$g_{\mathrm{HNC}/4}$	g_{MC}	f^2
0.805	0.0298	0.0282	0.0273	0.0065
0.865	0.1389	0.1331	0.1249	0.0363
0.925	0.3417	0.3310	0.3341	0.1035
0.985	0.6064	0.5927	0.5948	0.2139
1.045	0.8618	0.8490	0.8596	0.3517
1.105	1.064	1.056	1.066	0.4950
1.165	1.185	1.182	1.195	0.6254
1.225	1.244	1.246	1.245	0.7359
1.285	1.256	1.262	1.273	0.8231
1.345	1.234	1.241	1.268	0.8866
1.405	1.196	1.203	1.213	0.9326
1.465	1.150	1.158	1.167	0.9626
1.525	1.105	1.110	1.106	0.9815
1.585	1.062	1.066	1.062	0.9927

which equals the three-body contribution to U calculated with the lowest order g_3 given by the first diagram of Fig. 1 diagram 1.4. Differentiating F_{m1} in diagrams of type 3.2 in Fig. 3 will produce U diagrams included in the second term of the $g_{3,\mathrm{HNC}}$ in Fig. 1 diagram 1.4. In this way the $E_{\mathrm{JF}} - W$ calculated with the HNC g includes all the U diagrams calculated with $g_{3\mathrm{HNC}}$.

However, the $E_{\mathrm{JF}} - W$ calculated with HNC g also includes terms that correspond to improper g_3 diagrams. For example, differentiating the F_{m1} in Fig. 3 diagram 3.3 generates a U term in which the f_{n1}^2 in $g_{3,mn1}$ is approximated by unity. The f_{mn}^2, f_{n1}^2, and f_{m1}^2 in $g_{3,mn1}$ obviously can not be approximated. In order to obtain the correct U diagrams one must differentiate the sum of g_{mn} diagrams 3.3 and 3.4; but 3.4 is a HNC/4 diagram which is omitted when g_{HNC} is used to calculate the F_{JF}. This problem persists wherever the cluster expansion is truncated. Differentiating the F_{m3} in $g_{\mathrm{HNC}/4}$ diagram 3.5 will generate an inaccurate $g_{3,mn3}$ which can only be corrected by adding the derivative of diagram 3.6 which is a HNC/5 diagram.

TABLE II. Three-particle distribution function in HF at $\rho = 0.365\sigma^{-3}$. The r_{12}, r_{13}, and r_{23} are given in units of $\sigma = 2.556$ Å, while θ is in radians.

$r_{12} = r_{13}$	r_{23}	θ_{23}	$g_{3\,\mathrm{HNC}}$	$g_{3\,\mathrm{HNC}/4}$	$g_{3\,\mathrm{HNC}/4\,\mathrm{Super}}$
1.107	0.89	0.8274	0.235	0.118	0.2229
1.107	1.584	1.595	1.249	1.26	1.238
1.107	2.00	2.255	1.092	1.07	1.075
1.541	0.89	0.5859	0.2456	0.2349	0.2382
1.541	1.584	1.080	1.306	1.385	1.324
1.541	2.00	1.412	1.141	1.166	1.149
2.00	0.89	0.4488	0.1877	0.1791	0.1795
2.00	1.584	0.8143	0.9979	0.9774	0.9972
2.00	2.00	1.047	0.8724	0.8576	0.8655

TABLE III. Calculated energies of liquid ^{4}He.

$\rho(r^{-3})$	HNC	HNC/4	E_{KLV}	E_{SE}
0.283	−5.619	−5.669	−5.67	−6.13
0.341	−5.745	−5.836	−5.91	−6.77
0.365	−5.745	−5.836	−5.73	•••
0.4	−5.176	−5.325	−5.25	•••
0.416	−4.878	−5.045	−5.02	−6.67

IV. RESULTS

The two particle $g(r)$ in liquid ^{4}He at $\rho = 0.365$ atoms/σ^3 calculated with the HNC and HNC/4 approximations is compared with the exact Monte Carlo (MC) $g(r)$[12] in Table I. The standard Lennard-Jones potential[5] with $\sigma = 2.556$ Å is used in these calculations; and the f is constrained to heal at $d = 2r_0$. The difference between the HNC, HNC/4, and MC g's is quite small. Simple diagrammatic arguments given in the previous section suggested that one may expect

$$|g_{\mathrm{HNC}} - g_{\mathrm{HNC}/4}| > |g_{\mathrm{MC}} - g_{\mathrm{HNC}/4}| \,. \tag{4.1}$$

However the above inequality is not necessarily satisfied at all r; as a matter of fact the two differences have the same order of magnitude. This occurs because the terms in the expansion of g alternate in sign; the sign of the contribution of a diagram containing n F lines is simply $(-1)^n$ when $f^2 \leq 1$. Thus the sums of g diagrams belonging to any reasonable sequence are often much smaller than any individual diagram in the series.

The three-particle distribution functions in the above system calculated with the HNC and HNC/4 approximations are given in Table II. The last column in Table II gives the first term in $g_{3,\mathrm{HNC}/4}$ [Eq. (3.15)] which can be obtained by superposition. The differences between HNC and HNC/4 g_3's can be ≈0.1 and are somewhat larger than those between g_{HNC} and $g_{\mathrm{HNC}/4}$. The superposition approximation seems to be valid when r_{12}, r_{13}, r_{23} are all $>1\sigma$, but it overestimates g_3 when $r_{12} \approx r_{13} \approx r_{23} \leq 1\sigma$.

The calculated HF energies are given in Table III along with the best available variational estimates,[13] as well as available estimates from direct solutions of the many-body Schrödinger equation.[13] These calculations have been carried out at $d = 2r_0$. The convergence between the present HNC and HNC/4 is much better than that obtained by PB; the PB HNC/4 energies are too low, not so much because of their choice of E_{mn}, but mostly because of their neglect of the second term in $g_{3,\mathrm{HNC}/4}$ which gives a contribution of ≈0.3 °K at $\rho = 0.365\sigma^{-3}$. The Monte-Carlo calculation[12] at $\rho = 0.365$ with the $f(r, d = 2r_0)$ gives $E = -5.67 \pm 16$ °K in good agreement with the energies obtained from integral equations. The energies calculated with the pres-

TABLE IV. Hard sphere energies.

$\rho(a^{-3})$	$E(d=2r_0)$	$E(d=2.5r_0)$
0.166	4.296	4.295
0.2	5.985	6.032
0.244	8.719	8.872
0.27	10.65	10.84

ent f ($E_{\rm HNC}$ and $E_{\rm HNC/4}$) [Eq. (2.4)] are almost the same as those obtained with other variational calculations (E_{KLV}) which parametrize f and minimize E by varying each parameter. However all the variational energies are significantly above those (E_{SE}) estimated from solutions of the many-body Schrödinger equation.[13] The difference ($E_{\rm Jastrow} - E_{SE}$) represents the influence of the explicit many-body correlations neglected in the present work.

The $E(d)$ in both HF and HS systems becomes very insensitive to d when $d>2r_0$. PB discuss this result for HF, while in Table IV we give $E_{\rm HS}$ ($d=2$, $2.5r_0$), at various values of ρ, calculated by the HNC/4 method. The HS energies are in units of $\hbar^2/(ma^2)$.

The HS energies are compared with E_{KLV} and E_{SE}[13] in Table V. The approximations seem to be equally valid in HF and HS systems. The last two columns, $E_{LDE/2}$ and $E_{LDE/3}$, respectively, give the energies obtained with the first two and first three terms in the low-density expansion.[10] The expansion is valid only when $a/r_0 \ll 1$.

The $E(d>2r_0)$ is generally sensitive to d in the high-density Coulomb liquid. Table VI gives the $E(d)$ at $r_0=0.1$ and 0.01 in the units of the Bohr radius. The value of d/r_0 at which the energy has a minimum increases roughly like $r_0^{-1/4}$ for $r_0<1$ (Table VII). The calculated Coulomb energies compare favorably with the available low/high density limits[10]:

$$E_W(r_0 \gg 1) = -1.79 r_0^{-1} + 2.66 r_0^{-3/2},$$
$$E_B(r_0 \ll 1) = -0.803 r_0^{-3/4}. \tag{4.2}$$

Variational calculations of the Bose Coulomb liquid energy have also been carried out with the Monte Carlo method using an $f(r)$ given by an algebraic function with two parameters. These calculations are rather involved due to the long range of Coulomb correlations and, respectively, give -0.807 (-0.781) and -0.134 (-0.121) at $r_0=1$ and 10. The values given in parenthesis[12] are obtained with better numerical techniques than those used by Monnier.[14] The Monte Carlo energy at $r_0=10$ is in fair agreement with the present results, but at $r_0=1$ our f seems to underestimate the correlation energy by <10%. This is the most serious disagreement between the results obtained by the present method and the Monte-Carlo results.

A simple way to explain the variation of d/r_0 in the Coulomb system at high density is to appeal to the mean-field theory. The PB argument implies that the healing distance d is related to the range of the effective interaction. There are many methods to calculate the dielectric constant at high densities.[10] These methods are completely analogous to the random phase approximation in Fermi systems and give the Bogoliubov result E_B for the ground-state energy. The static dielectric constant is given by

$$\epsilon(q,0) = 1 + 12/r_0^3 q^4, \tag{4.3}$$

and the range of the effective two-particle interaction may be estimated as follows

$$v_{\rm eff}(r) = \sum_q e^{iqr} \frac{4\pi e^2}{q^2} \frac{1}{\epsilon(q,0)}$$
$$= \frac{e^2}{r} \exp[-(3/r_0^3)^{1/4} r] \cos[(3/r_0^3)^{1/4} r]. \tag{4.4}$$

The range of $v_{\rm eff}$ is clearly proportional to $r_0^{3/4}$, and thus d/r_0 should be proportional to $r_0^{-1/4}$. The effective interaction (4.4) is positive at small r and changes sign at

$$(3/r_0^3)^{1/4} r = (n+\tfrac{1}{2})\pi. \tag{4.5}$$

Due to the exponential the interaction beyond the second node is negligible, and hence we may estimate d in mean-field theory to be

$$\left(\frac{d}{r_0}\right)_{\rm MF} \approx \tfrac{3}{2}\pi \frac{r_0^{3/4}}{3^{1/4} r_0} = \frac{\pi}{2}\left(\frac{27}{r_0}\right)^{1/4}. \tag{4.6}$$

The calculated values of d (Table VII) are very

TABLE V. Hard sphere energies.

$\rho(a^{-3})$	a/r_0	HNC	HNC/4	$E_{\rm var}$	E_{SE}	$E_{LDE/2}$	$E_{LDE/3}$
0.24×10^{-6}	0.01	1.505×10^{-6}	...	...	...	1.504×10^{-6}	1.503×10^{-6}
0.24×10^{-3}	0.1	1.604×10^{-3}	...	...	...	1.612×10^{-3}	1.553×10^{-3}
0.166	0.866	4.327	4.296	4.32	4.15	3.089	−3.022
0.2	0.943	6.029	5.985	6.01	5.69	3.963	−3.988
0.244	1.01	8.970	8.719	8.80	8.14	5.179	−5.192

TABLE VI. Coulomb liquid energies with HNC equation.

d/r_0	$E(d, r_0=0.1)$	d/r_0	$E(d, r_0=0.01)$
5.2	−3.893	8.5	−22.6
6.0	−4.026	10	−24.44
6.4	−4.043	11.5	−25.11
6.8	−4.043	11.8	−25.11

close to the above estimate.

Figure 4 shows the variation of $f(r, d=d_{\min})$ in CL as the density is varied by a factor of $10^{12}(r_0 = 100-0.01)$. At low densities the Coulomb correlations resemble those due to a strong repulsive core, while at high ρ the correlation becomes weaker and longer (as compared to r_0) in range. The $f(r=0)$ approaches unity as $\rho \to \infty$, and that one can treat these different types of correlations over such a wide range of density with the HNC equation is very significant. As discussed in Sec. III it may be understood by noting that the elementary diagram expansion should converge due to fundamental constraints on the function G.

The present f neglects all the long-range correlations which influence the liquid structure function $S(k)$ at small k.[15] These long-range correlations may be included in a Jastrow wave function via a Reatto-Chester[15] term. Their effect on the HS energy has been estimated by Kalos, Levesque, and Verlet[13] at $\rho=0.2$ to be $\sim -0.1\hbar^2/ma^2$. It corresponds to ~1%–2% in high density HS. In principle it is possible to calculate the exact f in simple Bose systems by the method of paired phonon analysis developed by Feenberg and collaborators.[16]

The results reported in this section, and the NY results given in Ref. 17 verify the accuracy of the calculation of f from Eq. (2.4), and also that of energy with the HNC equation. That the variation of d/r_0 in high-density Coulomb system can be understood on the basis of conventional mean-field theory supports the arguments used by PB in obtaining Eq. (2.4). The energies obtained by the present method also satisfy the "upper-bound" property of a proper variational calculation.

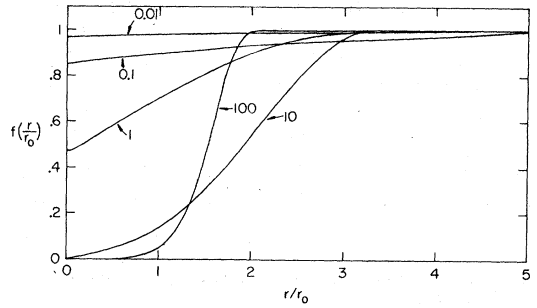

FIG. 4. $f(r/r_0)$ in CL at $r_0=100, 10, 1, 0.1, 0.01$.

V. SOLIDIFICATION CRITERION

Quantum liquids at zero temperature can solidify on compression (HS and HF), or on expansion (CL) or they may not solidify at all (NY) depending upon the two-body potential. Several criteria to predict the solidification density have been proposed; the most common are the Wigner,[18] Lindemann,[19] and the law of corresponding states.[20] These criteria are not very general, the first two have been useful in the CL system, while the last is for HF.

To obtain a general solidification criterion one may compare the variational energies in the liquid and solid phase.[21] This approach has been extensively used to study the solidification of HF, HS, and NY, and it is entirely numerical. In this section, we show that the comparison of liquid and solid energies becomes much simpler when one uses the present f in both the phases. For the sake of simplicity we consider a Boltzmann solid wave function:

$$\Psi_S = \prod_{i<j} f_{ij} \prod_i \phi_i , \tag{5.1}$$

$$\phi_i(r_i) = e^{-\nu(r_i-R_i)^2/2} . \tag{5.2}$$

Here R_i are the lattice points and f_{ij} is given by the Eq. (2.4). The ν is an additional variational parameter, and in the solid phase the $E(\nu)$ must have a minimum at a value of ν such that $\nu r_0^2 \gg 1$. Wave function (5.1) neglects the exchange symmetry which is thought to be unimportant in the

TABLE VII. Bose Coulomb energies.

	HNC/4			HNC			
r_0	E	(d/r_0)	$\left(\frac{d}{r_0}\right)_{MF}$	E	(d/r_0)	E_B	E_W
0.01	−25.64	13	11.32	−25.11	11.5	−25.39	•••
0.1	−4.003	6	6.37	−4.043	6.4	−4.516	•••
1	−0.722	3.4	3.58	−0.6968	3.35	•••	•••
10	−0.1261	2.5	•••	−0.1230	3.2	•••	−0.0949
100	−0.01421	2	•••	−0.01364	1.9	•••	−0.01524

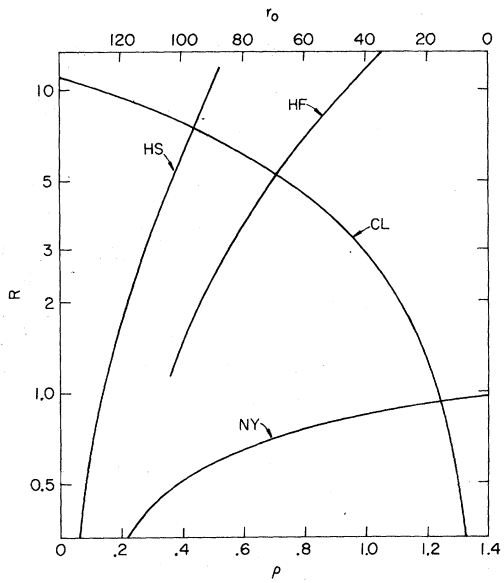

FIG. 5. Density dependence of the ratio R in various systems. The lower scale gives densities of HS, HF, and NY systems in units of a^{-3}, σ^{-3}, and fm^{-3}, respectively, while the top scale gives r_0 of the CL system.

solid phase.

The energy per particle of the solid can be written

$$E_S = W_S + T_S + U_S , \tag{5.3}$$

$$W_S = \frac{1}{2}\sum_{i\neq 1}\int g_S(\vec{r}_1,\vec{r}_i)V(r_{1i})\,d^3r_1\,d^3r_i , \tag{5.4}$$

$$T_S = \tfrac{3}{4}(\hbar^2/m)\nu , \tag{5.5}$$

$$U_S = \frac{1}{2}\frac{\hbar^2}{2m} \times \sum_{i\neq 1}\int g_S(\vec{r}_1,\vec{r}_i)\left(\frac{\nabla_1^2 f_{1i}}{f_{1i}} + \frac{(\nabla f_{1i})^2}{f_{1i}}\right) d^3r_1\,d^3r_i , \tag{5.6}$$

$$\left.\frac{\partial E_S(\nu)}{\partial \nu}\right|_{\nu=\nu_{eq}} = 0 , \tag{5.7}$$

and the $V(r)$ is given by Eq. (3.3). The two-particle distribution function $g_S(\vec{r}_1,\vec{r}_i)$ in solid phase is given by

$$g_S(\vec{r}_1,\vec{r}_i) \equiv \left(\int \Psi_S^2 \prod_{j\neq 1,i} d^3r_j\right) \Big/ \left(\int \Psi_S^2 \prod_j d^3r_j\right) . \tag{5.8}$$

Some useful properties of g_S can be obtained by noting that a sphere of radius $d \gg r_0$ will on the average contain $(d/r_0)^3$ particles. Thus when $d \gg r_0$

$$\int d^3r\, d^3r_1 \sum_{i\neq 1} g_S(\vec{r}_1,\vec{r}_i=\vec{r}_1+\vec{r}) = \left(\frac{d}{r_0}\right)^3 - 1 \qquad |r| \leq d . \tag{5.9}$$

Equation (5.9) is also valid in the liquid phase, and it can be used to obtain

$$W_S \approx \frac{\lambda}{2}\left[\left(\frac{d}{r_0}\right)^3 - 1\right] + \frac{\rho}{2}\int_d^\infty v(r) 4\pi r^2\, dr \approx W . \tag{5.10}$$

The solid energy is then given by

$$E_S = W + \frac{3}{4}\frac{\hbar^2}{m}\nu_{eq} + \frac{\hbar^2}{4m}\sum_{i\neq 1}\int g_S(r_1,r_i)\left(\frac{\nabla^2 f_{1i}}{f_{1i}} + \frac{(\nabla f_{1i})^2}{f_{1i}^2}\right) d^3r_1\,d^3r_i . \tag{5.11}$$

The W is obviously independent of ν, while the second term increases with ν. The last decreases as ν is increased, and it equals the liquid U at $\nu = 0$. One may crudely estimate the solid energy by assuming that the last two terms of (5.11) are comparable at ν_{eq}. In this case

$$E_S \approx W + \frac{3}{2}\frac{\hbar^2}{m}\nu_{eq} \gg W + \frac{3}{2}\frac{\hbar^2}{mr_0^2} . \tag{5.12}$$

Comparing E_S with the liquid energy suggests that solidification should occur when the dimensionless ratio R,

$$R = \frac{U(\rho)}{3\hbar^2/2mr_0^2} \tag{5.13}$$

becomes much greater than unity. Figure 5 shows R in the CL, HS, HF, and NY systems as calculated with f $(d = 2r_0)$. The R in HF and HS increases with ρ and thus these systems solidify at high ρ, while the R in the CL system, which melts at large ρ, decreases as ρ is increased. The R in NY system, which probably never solidifies,[9] increases with ρ at small ρ but reaches a rather

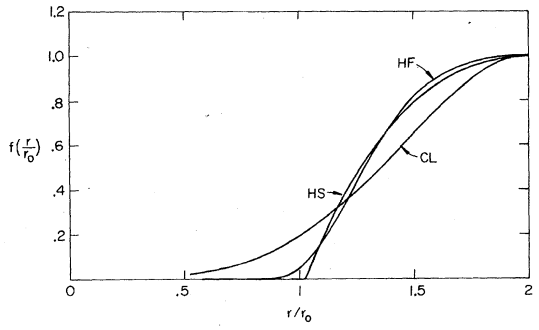

FIG. 6. The $f(r/r_0, d = 2r_0)$ in HS, HF, and CL systems at $R = 2.5$.

small maximum value ≈1 and finally decreases with ρ at very high densities.

It is easy to see that R depends only upon the dimensionless correlation $f(r/r_0)$, and thus two systems which have the same R have very similar correlations. The similarity between correlations in HS ($\rho = 0.25a^{-3}$), HF ($\rho = 0.51\sigma^{-3}$), and CL ($r_0 = 35$) at densities (given in parenthesis) at which $R = 2.5$ is shown in Fig. 6. The HS and HF systems solidify when R becomes ≈2.5, and on the basis of the present criteria one would expect the Coulomb system to melt at $r_0 \approx 35$. A direct comparison[22] of the variational CL liquid energy with the harmonic solid energy suggests $r_0 = 360$ at melting. However this value decreases to $r_0 = 120$ if[22] the solid energy is estimated in the Hartree approximation. The value may further decrease on considering the effect of short-range correlations on the CL solid energies.

ACKNOWLEDGMENTS

The authors are most indebted to Professor G. V. Chester for carrying out the Monte Carlo calculation of HF with the present f, and also for communicating the more recent results on the CL system. A part of this work was carried out while one of the authors (VRP) visited the Tata Institute of Fundamental Research, Bombay, India.

---

*Supported by NSF MPS-74-22148.

[1]D. Schiff and L. Verlet, Phys. Rev. 160, 208 (1967).
[2]V. R. Pandharipande and N. Itoh, Phys. Rev. A 8, 2564 (1973).
[3]M. L. Ristig, W. J. Terlouev, and J. W. Clark, Phys. Rev. C 3, 1504 (1971), 5, 695 (1972).
[4]V. R. Pandharipande and R. B. Wiringa, Nucl. Phys. A 266, 269 (1976).
[5]V. R. Pandharipande and H. A. Bethe, Phys. Rev. C 7, 1312 (1973).
[6]J. M. J. van Leeuwen, J. Groeneveld, and J. deBoer, Physica (Utr.) 25, 792 (1959).
[7]R. D. Murphy and R. O. Walts, J. Low Temp. Phys. 2, 507 (1970).
[8]H. W. Jackson and E. Feenberg, Ann. Phys. (N.Y.) 15, 266 (1961).
[9]D. M. Ceperily, G. V. Chester, and M. H. Kalos (unpublished).
[10]A. L. Fetter and J. D. Walecka, *Quantum Theory of Many-Particle Systems* (McGraw-Hill, New York, 1971).
[11]R. A. Smith, Phys. Lett. B (to be published).
[12]G. V. Chester (private communication).
[13]M. H. Kalos, D. Levesque, and L. Verlet, Phys. Rev. A 9, 2178 (1974).
[14]R. Monnier, Phys. Rev. A 6, 393 (1972).
[15]L. Reatto and G. V. Chester, Phys. Lett. 22, 276 (1966).
[16]C. E. Campbell and E. Feenberg, Phys. Rev. 188, 396 (1969).
[17]V. R. Pandharipande, Nucl. Phys. A 248, 524 (1975).
[18]E. P. Wigner, Phys. Rev. 46, 1002 (1934); Trans Faraday Soc. 34, 678 (1938).
[19]D. Pines, *Elementary Excitations in Solids* (Benjamin, New York, 1963).
[20]J. deBoer, Physica (Utr.) 14, 139 (1948).
[21]J. P. Hansen and D. Levesque, Phys. Rev. 165, 293 (1968).
[22]J. P. Hansen, B. Jancovici, and D. Schiff, Phys. Rev. Lett. 29, 991 (1972).